PHILOSOPHICAL TRANSACTIONS OF THE ROYAL SOCIETY A MATHEMATICAL, PHYSICAL & ENGINEERING SCIENCES

Simulations Using Hard Particles

Michael P. Allen

Phil. Trans. R. Soc. Lond. A 1993 **344**, 323-337
doi: 10.1098/rsta.1993.0093

Simulations using hard particles

By Michael P. Allen

H. H. Wills Physics Laboratory, Royal Fort, Tyndall Avenue, Bristol BS8 1TL, U.K.

A short review is given of recent progress in the computer simulation of liquid crystal phases using hard particles. Emphasis is placed on the richness of phase behaviour that may result from the effects of molecular size and shape alone, and on the role of simulations in testing modern theories of liquid crystal phase transitions, structure and dynamics. Two specific examples are treated in detail: the simulation of twisted nematic liquid crystals, allowing a direct calculation of the twist elastic constant and the helical twisting power of chiral dopant molecules; and the recent quantitative explanation of diffusive behaviour in isotropic and nematic liquids using kinetic theory.

1. Introduction

Computer simulations provide one of the most helpful tools to aid, and test, our understanding of condensed-matter systems. The basic aim is to relate molecular shapes, sizes and interactions to the observed bulk properties. A perfect theory would do this, and essentially 'explain' what we see in experiment: an approximate theory still provides much insight. The role of simulation is to help discriminate between good theories and bad ones, and shed some light on the reasons for success and failure. To do this, it is not necessary to model intermolecular interactions precisely: this would be very difficult, expensive, and, in the end, not very illuminating. The situation is especially severe for liquid crystals: the molecules are quite complicated, having flexible or semi-flexible structures, and often possessing interesting electronic charge distributions leading to electrostatic forces and significant polarizability anisotropies. Moreover, in these systems, the characteristic phenomena occur over long time scales and length scales. At present, we wish to establish rather general relationships between simple molecular parameters and observed properties. Accordingly, several groups have concentrated on simple, rigid, hard-particle models, and on rigid-body models incorporating some simple attractive forces, but ignoring the subtleties of 'realistic' potentials. This paper concentrates on the former category.

Hard spheres are known to provide a firm base for the study of the statistical mechanics of simple atomic liquids (Hansen & McDonald 1986); we expect them to be a good guide for molecular fluids in general. Any theory which can explain the tricky, entropic part of the free energy of a liquid, due principally to molecular excluded-volume effects, should be easy to extend to cope with attractive forces. The principles of this approach are well established. Furthermore, it has been known for many years (Onsager 1949; see also de Gennes 1974; Frenkel 1987) that orientational ordering will be seen when the density of a system of needlelike hard bodies, or indeed thin platelike ones, increases beyond a critical (shape-dependent) value. Thus, the most important feature of the systems of interest (orientational ordering) is present

Phil. Trans. R. Soc. Lond. A (1993) **344**, 323–337
Printed in Great Britain

for these models. Of course, other features of self-assembly, which may depend upon attractive interactions, may be absent.

Certain classes of theory are well developed for such simple systems. For hard particles, we especially wish to test the density-functional, van der Waals–Onsager theories described in the previous paper, which should predict the position of phase transitions, variation of order-parameters with state point, and other static properties. We are also interested in kinetic theories for transport coefficients and other dynamical properties. Both methods have been extensively tested on the hard sphere fluid, and their advantages and limitations in this area are well known.

In this paper I cannot give a comprehensive review even of this limited field of hard-particle simulation, and must refer the reader elsewhere (Allen *et al.* 1993). In the following sections I briefly summarize the simulation techniques used, describe some of the liquid crystal phases observed, and then give some examples of recent progress. I conclude with a look to the future.

2. Simulation methods

Simulations of liquid crystals and other complex fluids are essentially no different from those of simple liquids that have been carried out over the past 35 years (Ciccotti *et al.* 1987). The basic techniques are relatively straightforward to implement (Allen & Tildesley 1987). Monte Carlo (MC) simulations of hard particles are particularly simple. One attempts to move each particle in turn, translating it and rotating it by small amounts. Such a trial move is selected using a random number generator, rejected if it would lead to overlap of the selected particle with any other, and accepted if no overlaps result. This requires efficient evaluation of a pair overlap criterion: a function F of the orientations and positions of any pair of molecules, which takes values $F < 1$ if they overlap, $F > 1$ if they do not, and $F = 1$ at contact. Efficient prescriptions exist (Vieillard-Baron 1972, 1974; Perram *et al.* 1984; Perram & Wertheim 1985) to determine F for simple shapes like spherocylinders and spheroids. Variants of the MC prescription conveniently generate states sampled from the constant-NVT ensemble (where N is the number of particles, V the sample volume and T the temperature), the constant-NPT ensemble (P is the pressure), and so on.

Hard-particle molecular dynamics (MD) is a little more complicated. The aim is to solve Newton's equations of motion. For each hard particle, this means free flight with constant linear and angular momenta, in between impulsive collisions with other particles. Having dealt with one collision, the aim is to locate the next: this involves considering, in principle, every pair of particles, calculating the time at which they are due to collide, and selecting the next collision in chronological order. At the point of collision, impulsive forces determined by the conservation laws and the contact condition (i.e. whether the colliding surfaces are rough or smooth) dictate the post-collisional momenta. Both free flight and collision dynamics also depend on the choice of molecular masses and moments of inertia. The technique requires efficient evaluation of the pair overlap function F and its time derivative $\dot{F}$, so as to locate the exact time of collision for each pair by standard root-finding methods (e.g. Newton–Raphson). This type of approach has been implemented for a variety of molecular shapes (Rebertus & Sando 1977; Allen *et al.* 1989). Typically, the constant-NVE ensemble is probed, where E is the energy, although constant-NVT and -NPT methods are easy to devise.

Simulations yield simple thermodynamic quantities like the pressure, orientational and positional order parameters, and structural features like the pair distribution function. Additionally, MD simulations yield dynamical quantities like the velocity autocorrelation function, which may be used to calculate the diffusion coefficient. The observation of diffusive behaviour is additional evidence for an ordered *fluid* phase, rather than a crystalline or glassy solid state. To characterize different phases, we are most interested in the calculation of order parameters and free energies. Orientational ordering is measured, in the simple case of a nematic phase, by $S \equiv \langle P_2(\cos\theta)\rangle$; here $\langle \ldots \rangle$ denotes a simulation average, P_2 is the second Legendre polynomial and $\cos\theta = \boldsymbol{u}\cdot\boldsymbol{n}$ where θ is the angle between a typical molecular axis $\boldsymbol{u}$ and the preferred direction in space, the *director* $\boldsymbol{n}$. The location of the director, and the evaluation of S, amounts to a simple eigenvalue problem (Zannoni 1979; Eppenga & Frenkel 1984). However, a useful check is to measure the orientational correlation function $g_2(r) \equiv \langle P_2(\boldsymbol{u}(0)\cdot\boldsymbol{u}(r))\rangle$ between molecular orientation vectors $\boldsymbol{u}$ on molecules a distance r apart. In an isotropic phase this function decays to zero within a few molecular diameters, but in an ordered phase it reaches a long-range non-zero value $g_2(r\to\infty) = S^2$.

Free energies are calculated by thermodynamic integration from well-characterized state points, or (for low densities only) by Widom's test-particle insertion method (Widom 1963). (For more details of free-energy calculations in this context see (Eppenga & Frenkel 1984; Frenkel 1986; Stroobants *et al.* 1986; Veerman & Frenkel 1992).) The observation of order-parameter variation with state point gives a rough-and-ready guide to the phase diagram; typically 50–100 different simulations will be needed to cover the range of variation of two parameters (for example, density and molecular elongation) for a family of simple molecular shapes. Each run might take a few hours of CPU time.

It is as well to bear some limitations in mind. Typically, the cost of computer time restricts us to rather small systems ($O(10^3)$ particles) and relatively short runs ($O(10^4)$ MC moves per particle or MD collisions per particle). Periodic boundary conditions are used to eliminate surface effects, and make the effects of finite-size fairly small. For nematic phases, there seems to be little evidence that periodic boundaries have a significant influence on measured properties, in particular on the direction and magnitude of the orientational ordering. For smectics and columnar phases, on the other hand, it is important to allow the box dimensions to vary, so as to accommodate the long-ranged structural order. In general, the study of different system sizes is very desirable, but few groups have sufficient computer power to conduct thorough investigations of this kind.

The limitations on run length become most important if the precise location and characterization of phase transitions is required. The essential problem is that, in many cases of interest, the transitions are weakly first order or continuous. Recall that a first-order transition occurs when the free energies of the two phases become equal; around this point there is a discontinuous variation in properties such as the energy, the density, and the order parameter characterizing the transition. However, either phase may be metastable, so that the corresponding branch of the equation of state will extend beyond the transition point. Consequently, the free energy calculation is essential to locate the point of thermodynamic coexistence. In a simulation, one looks for the intersection of two chemical potential curves as functions of, say, pressure, at constant temperature. The gradients of these curves will be different at the transition point, where they intersect; for a weak transition,

PHILOSOPHICAL TRANSACTIONS OF THE ROYAL SOCIETY A MATHEMATICAL, PHYSICAL & ENGINEERING SCIENCES

the curves become nearly parallel and it is difficult to locate the transition accurately. For a continuous transition, the curves join smoothly; instead of discontinuous changes, one sees a divergence in order-parameter fluctuations at the transition. It is possible to analyse the system-size dependence of these effects for both continuous and first-order transitions; indeed, this is the essential tool in characterizing phase transitions by simulation (Mouritsen 1984; Binder & Stauffer 1987; Allen 1993*a*). A precise determination of the liquid–crystal transition point involves very lengthy runs, and the careful accumulation of distribution functions of the order parameter, or related quantities. Recent studies of lattice models of liquid crystals (Zhang *et al.* 1992; Cleaver & Allen 1993) indicate that run lengths of order 10^6 MC moves/particle are needed to do this properly. For hard-particle systems, and indeed for atomic and molecular simulations in general, runs of such length can only rarely be undertaken; one recent example is a study of the critical point in the two-dimensional Lennard–Jones atomic system (Wilding & Bruce 1992). Accordingly, we have only a crude picture of the phase diagrams for liquid crystal systems modelled using particles.

3. Hard particle mesophases

In this section we examine four classes of hard-particle model, with the intention of highlighting the diversity of phase behaviour exhibited even by such simple potentials. This list is not intended to be exhaustive, but simply to offer examples of current research. For almost all of these models we describe the phase diagram in terms of a single shape parameter γ, which measures the ratio of the molecular length to its width, and a reduced density $\rho^* = \rho/\rho_{cp}$ where ρ_{cp} is the density of closest regular packing.

(*a*) *Spheroids*

One of the simplest shapes studied to date is the spheroid: a sphere subjected to elongation or compression, possibly by different factors, in mutually perpendicular directions. Defining the semi-axes ('radii') to be a, b and c, we distinguish two cases: axially symmetric molecules, $a \neq b = c$ (ellipsoids of revolution), and general biaxial molecules with $a \neq b \neq c$.

In the axially symmetric case, γ is simply the axial ratio or elongation $e = a/b$. For suitably extreme values $e \gg 1$ and $e \ll 1$, there is a nematic liquid crystal in which the symmetry axes are aligned, in addition to an isotropic fluid and fully ordered solid phase. The regions of nematic stability have been established by Monte Carlo simulation with free energy calculation, by Frenkel and co-workers, for $e = 1/3$, $1/2.75$, 2.75, 3 (Frenkel *et al.* 1984; Frenkel & Mulder 1985). For less extreme axial ratios, no nematic phase is seen. For values $e \approx 1$ around the well-known hard-sphere model, a plastic crystal phase (with rotational disorder) is present, but this has hardly been studied, and is not our concern here. Using these results, and the known Onsager limit, a global phase diagram could be inferred. This is illustrated in figure 1, where we show both the oblate and prolate branches.

More extreme shapes, $e = 1/10$, $1/5$, 5, 10 have been studied (Allen & Wilson 1989), although free energy calculations have not been attempted in these cases; the transition points were estimated from the order-parameter variation. These points are also shown on the figure. In all these cases, *spontaneous* ordering to form the nematic phase is seen on uniformly compressing the isotropic phase through the transition density. It is not necessary to apply an external field. As the system is compressed beyond the limit of thermodynamic stability of the disordered phase, it

PHILOSOPHICAL TRANSACTIONS OF THE ROYAL SOCIETY A MATHEMATICAL, PHYSICAL & ENGINEERING SCIENCES

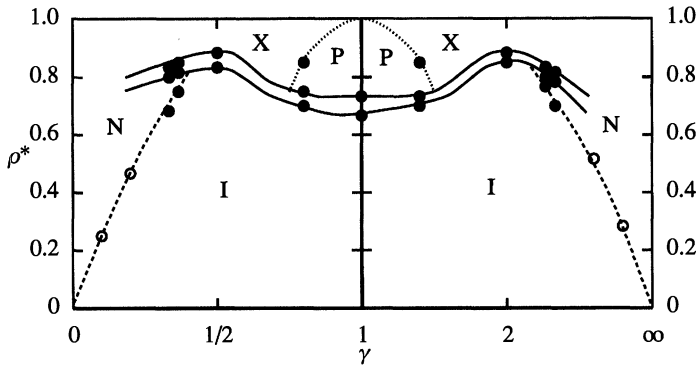

Figure 1. Phase diagram of oblate and prolate axially symmetric spheroids (schematic). The horizontal axis is the axial ratio $e = a/b$, on a scale which highlights the $e \leftrightarrow e^{-1}$ relation. The vertical scale is the reduced density ρ^*. Filled circles denote phase transitions located by free energy calculations, open circles those located by other means. Solid lines delimit the melting transition coexistence region, while dashed lines mark the other transitions (for which the coexistence regions are small or nonexistent). Phases are: I, isotropic fluid; N, nematic; X, crystal; P, plastic crystal. (After Frenkel & Mulder 1985; see also Allen & Wilson 1989.)

at first follows a metastable extension of the isotropic liquid equation of state, before jumping over to the nematic branch.

The phase diagram is strikingly symmetrical with respect to the oblate $\leftrightarrow$ prolate transformation $e \leftrightarrow 1/e$. This symmetry is expected at low densities because the second virial coefficient $B_2(e)$ equals $B_2(1/e)$. However, no such relation holds between the third and higher virial coefficients. Indeed, for more extreme shapes, there are systematic differences in the equations of state and on the phase diagram: the platelike systems are slightly more aligned at a given density than the corresponding needlelike ones, and the nematic phase seems to extend to lower densities.

The exact values of e at which the nematic phase is 'squeezed' out between isotropic liquid and solid, on the oblate and prolate sides of the diagram, are not clear at present. Indeed, there may be some system-size effects on the phase transition, which require further study. It has been reported (Zarragoicoechea *et al.* 1992) that the $e = 3$ nematic phase, observed by Frenkel & Mulder for system sizes $N \sim 100$, disappears when $N = 256$, for densities $\rho^* < 0.76$. However, we have also observed spontaneous ordering, using both MD and MC methods, for systems of this size, at $\rho^* < 0.76$ (C. P. Mason & M. P. Allen 1993, unpublished work). Whatever the reason for the discrepancy, it highlights the possibility of finite-size effects, and/or simulation box shape effects, on phase transitions. Clearly, a more extensive study is needed here, but it should be stressed that, regardless of the outcome for this particular value of e, the general features of the phase diagram in this region are not in doubt.

The isotropic–nematic transition for hard ellipsoids of $e \approx 3$ seems to be weakly first order (Frenkel *et al.* 1984; Frenkel & Mulder 1985), i.e. the density jump is relatively small, *ca.* 2%. As the shape becomes more elongated, we expect to see progressive strengthening, towards the Onsager limit where the density jump is *ca.* 20%. Nematic precursor fluctuations, the slow collective molecular reorientations that herald the onset of nematic ordering, have also been observed for $e = 3$ (Allen & Frenkel 1987). Thus, although not studied in detail, the transition has the basic features observed in experiment.

PHILOSOPHICAL TRANSACTIONS OF THE ROYAL SOCIETY A MATHEMATICAL, PHYSICAL & ENGINEERING SCIENCES

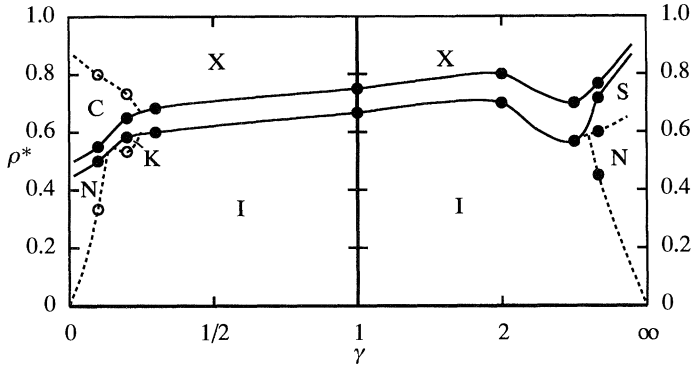

Figure 2. Phase diagrams of cut spheres and spherocylinders (schematic), to compare with the spheroid diagram of figure 1. The horizontal axis is the length-to-width ratio $\gamma = L/D$ for cut spheres, $\gamma = (L+D)/D$ for spherocylinders. The vertical scale is the reduced density ρ^*. Notation as for figure 1. Phases are: I, isotropic fluid; N, nematic; S, smectic; X, crystal; C, columnar; K, cubatic. A plastic crystal phase presumably appears at high density around $\gamma \approx 1$, but this has not been studied to date. (After Veerman & Frenkel 1990; Veerman & Frenkel 1992.)

Molecules having unequal axes $a \neq b \neq c$, intermediate in shape between rods and discs, may additionally show a biaxial nematic phase. For the family of shapes $c/a = 10$, $1 \leqslant b/a \leqslant 10$, a rough survey of the phase diagram has been carried out (Allen 1990*a*). This entailed the calculation of uniaxial and biaxial order parameters, but no free energy calculations have been performed to date. The biaxial phase seems to lie very close to the critical value $b/a \approx \sqrt{10}$ predicted by the simplest theories, and to be stable for only a rather narrow range of shapes around this value. Once more, there is an approximate symmetry in the phase diagram corresponding to rodlike $\leftrightarrow$ platelike interconversion $\{a, b, c\} \leftrightarrow \{c, ca/b, a\}$. This system is of interest for a second reason: it may shed light on the influence of molecular biaxiality on the strength of the I $\leftrightarrow$ N transition. This is expected to weaken significantly as one departs from the axially symmetric limit, and this would partly reconcile the discrepancy between the extremely weak transitions seen in experiment and the rather stronger ones predicted by theory in the axially symmetric case. This effect is predicted by the theories discussed in the previous paper, and confirmation by simulation would be very welcome. To date, however, simulations of sufficient length have not been performed, and we anticipate that this will be quite a challenge.

(*b*) *Spherocylinders*

A prolate molecule may be modelled by a spherocylinder, i.e. a cylinder of length L, diameter D, with hemispherical caps of diameter D at each end. The overall length-to-width ratio is therefore $\gamma = (L+D)/D$. Simulations of spherocylinders with $L/D = 5$ (Frenkel 1988; Frenkel *et al.* 1988) revealed the presence of a nematic phase which becomes stable relative to the isotropic liquid at about $\rho^* \approx 0.45$, and then a smectic phase for $0.6 \lesssim \rho^* \lesssim 0.75$, where the solid appears. This work was recently extended to other aspect ratios (Veerman & Frenkel 1990). These authors observed metastable nematic ordering at $L/D = 3$, but concluded that no ordered fluid phases were thermodynamically stable for this shape. They proposed that an isotropic–smectic–solid triple point exists for $L/D \gtrsim 3$, and a second, isotropic–nematic–smectic triple point exists for a shape somewhere in the range $3 < L/D < 5$. The tentative phase diagram is illustrated schematically in figure 2.

It may seem surprising that pure rigid-body excluded-volume effects can give rise

to smectic ordering; more obvious arguments are based on molecular attractions favouring a side-by-side arrangement, or on the effects of flexible tails. However, theoretical predictions of thermodynamically stable hard-core smectics have now appeared, as discussed in the previous paper.

MD simulations by Frenkel and co-workers have revealed the time-dependent smectic precursor fluctuations which occur as the nematic–smectic transition is approached from the nematic side. The dynamical technique has also allowed a comparison of diffusion coefficients parallel to the smectic layer planes, corresponding to motion within layers, and in the perpendicular direction, corresponding to interlayer motion. Further details can be found elsewhere (Allen *et al.* 1989). As in the case of ellipsoids, there are no dramatic, qualitative discrepancies between the properties of hard spherocylinders and those of real liquid crystals.

(*c*) *Truncated spheres*

An oblate molecule may be modelled by slicing the top and bottom off a sphere using two parallel cuts. This model is defined by a length-to-width ratio $\gamma = L/D < 1$, D being the sphere diameter, and L being the distance between the parallel flat surfaces. The cases $L/D = 0.1, 0.2, 0.3$ have been studied (Veerman & Frenkel 1992).

For the system with $L/D = 0.1$ it was observed that the system spontaneously ordered to form a nematic phase at $\rho^* \approx 0.33$. At $\rho^* \approx 0.5$, this nematic phase undergoes a strong first-order transition to a columnar phase, with a density roughly 10% higher. The columnar–crystalline transition occurs at much higher density ($\rho^* \gtrsim 0.8$).

The situation for $L/D = 0.2$ seems to be more complicated. This undergoes a transition at $\rho^* \approx 0.5$ to a phase having no long-range (second-rank) nematic order, as measured by the orientational correlation function $g_2(r)$ which is very short ranged, and by the order parameter $S = \langle P_2 \rangle$. However, the higher-order orientational correlation function $g_4(r) \equiv \langle P_4(\boldsymbol{u}(0) \cdot \boldsymbol{u}(r)) \rangle$ is much longer ranged than $g_2(r)$, indicating cubic-symmetry orientational correlations. The resultant phase is termed 'cubatic' (not to be confused with 'cubic', which refers to a system that also has *translational* order). This four-fold orientational ordering results from the packing of short(ish) columns of particles against each other, with frequent 90° angles. Simulations (Veerman & Frenkel 1992) using system sizes up to $N = 2048$ indicate that, at least for the model with $L/D = 0.2$, the cubatic phase may be thermodynamically stable over a narrow density range, and is certainly metastable over a wider range. Whether stable or metastable, it provides an elegant example of molecular self-assembly in the absence of attractive forces.

Both nematic and cubatic phases seem to be absent for $L/D = 0.3$, and one observes direct conversion of isotropic fluid into solid. Very close to the hard-sphere limit $L/D \to 1$ there is, presumably, a plastic crystal phase, but this has not been studied to date. The tentative phase diagram appears in figure 2.

(*d*) *Flexible chains*

Very recently, a study has been conducted of semi-flexible chains of hard spheres (Wilson & Allen 1993). The aim was to complement other studies of linear, rigid chains (Whittle & Masters 1991; Amos & Jackson 1992), and begin to understand the role of molecular flexibility on the position of phase transitions and the characteristics of the orientationally ordered phases. Restricted chain stretching and bending was permitted, by applying hard repulsive and attractive potentials to the intramolecular

interactions. An MD method was used, in which the atoms rattle together, restrained by hard constraints on bond lengths. The simulations were conducted at constant pressure (i.e. system volume changes were attempted at regular intervals according to the usual MC prescription). For a system of molecules composed of seven touching hard spheres ($\gamma \approx 7$) a nematic phase appeared at $\rho^* \approx 0.4$, and a smectic phase formed at $\rho^* \approx 0.55$. Interestingly, the smectic layers, although unambiguous, turned out to be much less sharply defined than in the analogous case of spherocylinders with $L/D = 5$ (i.e. $\gamma = 6$). However, a direct comparison may not be strictly appropriate, in view of the different length-to-width ratio and the slightly lower density of the hard-sphere system.

4. Simulated properties

Here we select static and dynamic properties, characterizing the nematic phase, calculated by simulation with the intention of testing theories and of pointing the way to useful comparison with experiment. Again, we cannot aim to be comprehensive. Two examples are picked out and treated in a little more detail to give the flavour of current research: the calculation of the helical twisting power for chiral molecules dissolved in a nematic solvent, and the explanation, by kinetic theory, of some interesting diffusive behaviour in the nematic phase.

(a) *Static properties*

The variation of the order parameter with density in the nematic phase, and the position of the isotropic $\leftrightarrow$ nematic transition, are the simplest criteria for comparison of theory with simulation. Comparisons of S with the predictions of an Onsager-like theory based on second and third virial coefficients, for axially symmetric spheroids, has been made (Tjipto-Margo & Evans 1990). The inclusion of the third-order term seems to dramatically improve the quantitative agreement between theory and simulation, as well as permitting an explanation of the loss of $e \leftrightarrow 1/e$ symmetry. This type of theory (see Tarazona, this volume) is equivalent to making an approximation to the direct correlation function $c^{(2)}$.

These same theories are capable of predicting the values of the Frank elastic constants, which determine the response of the system to any external perturbation causing an orientational deformation. These quantities may also be related to the direct correlation function. In the simplest case of the nematic phase, the free energy of deformation may be written (de Gennes 1974)

$$\Delta\mathscr{F} = \frac{1}{2}\int \mathrm{d}\boldsymbol{r}\{K_1(\nabla\cdot\boldsymbol{n})^2 + K_2(\boldsymbol{n}\cdot(\nabla\wedge\boldsymbol{n}))^2 + K_3(\boldsymbol{n}\wedge(\nabla\wedge\boldsymbol{n}))^2\},$$

which essentially defines the splay, twist and bend elastic constants, K_1, K_2 and K_3 respectively. One route to these quantities, in a simulation, is to study equilibrium orientational fluctuations as functions of wave vector $\boldsymbol{k}$. The relevant expressions are valid for small but finite $k = |\boldsymbol{k}|$, and of course $\boldsymbol{k}$ must be chosen commensurate with the simulation box: a tedious (and possibly error-prone) extrapolation to low k is required in practice. Comparisons of theory and simulation have been made for ellipsoids and spherocylinders (Allen & Frenkel 1988; Allen & Frenkel 1990; Somoza & Tarazona 1989; Tjipto-Margo *et al.* 1992); in all cases the results are comparable, but theory systematically underestimates the simulation results. (Some confusion on this point was caused by an error of a factor of $\frac{9}{4}$ in the original papers (Allen &

PHILOSOPHICAL TRANSACTIONS OF THE ROYAL SOCIETY A MATHEMATICAL, PHYSICAL & ENGINEERING SCIENCES

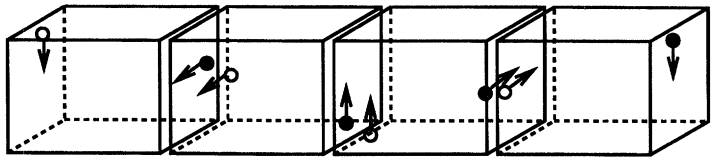

Figure 3. Twisted periodic boundary conditions used to stabilize twisted nematic phase. We show four identical copies of the simulation box, each rotated by $\pm\frac{1}{2}\pi$ with respect to its neighbours. Two particles (one black, one white) each with an arrow to indicate orientation, are shown to illustrate the effects of the rotation.

Frenkel 1988; Allen & Frenkel 1990).) Recall that these same theories are comparatively successful in reproducing the transition density and order-parameter variation, as mentioned above. This discrepancy may be due to the sensitivity of the elastic constants to the variation of the direct correlation function $c^{(2)}$ at larger separations, outside the hard-core overlap region. However, it is also possible that the simulation results are at fault, through system-size effects, problems with extrapolating to low k, and so forth. In any case, a more detailed knowledge of the form of $c^{(2)}$ for both isotropic and nematic molecular liquids would be helpful in understanding more about these quantities.

Very recently, a more direct approach has been made (Allen & Masters 1993) to calculating the twist elastic constant K_2, by directly measuring the torque density in a system of molecules in twisted periodic boundary conditions. For a cuboidal simulation box of dimensions $L_x = L_y \neq L_z$, periodic replicas in the $\pm z$ direction are rotated by, respectively, $\pm\frac{1}{2}\pi$ about the z axis relative to the original. This rotation is applied to centre-of-mass coordinates as well as molecular orientations, but for a nematic fluid the distortion of the positional degrees of freedom is inconsequential. One full turn of the orientational distribution is thus effectively implemented over four box lengths in the z direction, as shown in figure 3.

A uniformly twisted nematic director field,

$$\boldsymbol{n}(\boldsymbol{r}) = (\cos\phi(z), \sin\phi(z), 0), \quad \mathrm{d}\phi/\mathrm{d}z = k = \text{const.},$$

with the director everywhere perpendicular to the z axis, of wave vector $k = 2\pi/\lambda = \pi/2L_z$, is stabilized in these boundaries. The twist elastic free energy is

$$\Delta\mathscr{F} = \tfrac{1}{2}VK_2k^2$$

and associated with this is an internal torque density, rather like the internal pressure which is present in any system confined within periodic boundaries. Measurement of the torque density gives the twist elastic constant K_2. Preliminary estimates of K_2, for $e = 5$ and $e = 10$ prolate ellipsoids of revolution, give the expected density dependence, and values roughly consistent with (if slightly lower than) the same quantities measured by fluctuation methods, but more extensive studies of system-size and k-dependent effects are needed before firm conclusions are drawn. This remains an active area of research.

Finally in this section, we discuss chiral nematic, or cholesteric, phases, characterized by the twisted director field which results when small concentrations of chiral (left- or right-handed) dopant molecules are added to a nematic phase. In the presence of such chiral dopants, the twist free energy becomes (de Gennes 1974)

$$\Delta\mathscr{F} = \tfrac{1}{2}VK_2(k-k_0)^2.$$

PHILOSOPHICAL TRANSACTIONS OF THE ROYAL SOCIETY A MATHEMATICAL, PHYSICAL & ENGINEERING SCIENCES

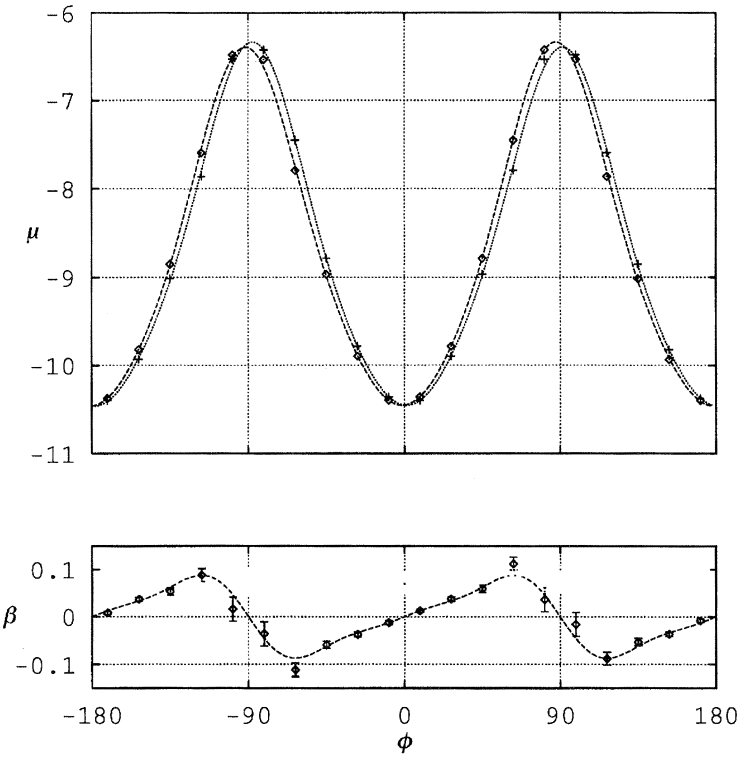

Figure 4. The chemical potential as a function of twist angle, $\mu(\phi)$, for an X-shaped ellipsoid dimer (dashed line) and its mirror-image function $\mu(-\phi)$ (dotted line). The absolute position of the vertical scale is arbitrary. Below, the helical twisting power $\beta(\phi)$ obtained from the difference between these functions.

At low dopant concentrations there is a linear relation between concentration and equilibrium wavenumber k_0, written conventionally as $k_0 = 2\pi/\lambda = 4\pi\beta\rho$ where $\rho = N/V$ is the number density of dopant molecules. The constant of proportionality, β, has the dimensions of area, and is termed the *helical twisting power*. At first sight, the calculation of β seems very difficult. Typical values of the helix pitch, for dopant concentrations of a few percent, are comparable with the wavelength of visible light, far larger than accessible system sizes in molecular simulations using $N \approx 1000$ particles. The requirement to avoid unphysical surface effects by using periodic boundary conditions means that the helix pitch must be commensurate with the simulation box length. High concentrations of dopant would be needed to produce such pitches, but the definition of β is only valid in the dilute régime. Clearly, the properties of a nearly pure liquid of chiral molecules will be quite different from those of a dilute solution. In experiment, more exotic phases (the 'blue' phases) may be formed as the dopant concentration increases, so it may not be at all relevant to study a small, highly concentrated sample, in any case. Moreover, we anticipate that very long simulation timescales would be needed to establish the equilibrium helix pitch for a given composition of liquid.

We have recently demonstrated that the helical twisting power β can, in fact, be measured in a simulation using the twisted boundary conditions described above (Allen 1993*b*). In the very simple case where the chiral dopants are composed of two hard-ellipsoidal monomer units, in a scissors arrangement, dissolved in a hard

PHILOSOPHICAL TRANSACTIONS OF THE ROYAL SOCIETY A MATHEMATICAL, PHYSICAL & ENGINEERING SCIENCES

ellipsoid solvent, one merely needs to simulate the monomer ellipsoid system. For a more general chiral dopant, a single molecule dissolved in the nematic solvent is needed. The method amounts to an accurate calculation of the chemical potential difference $\mu_L - \mu_R$ between mirror-image left- and right-handed dopant forms in a uniformly twisted nematic phase of fixed pitch. This structure is stabilized by conducting the simulation in the twisted periodic boundary conditions just described. The chiral dimer is representative of a class of molecules actually synthesized and studied experimentally, and known to have very high values of β (Heppke *et al.* 1986; Heppke *et al.* 1990). In figure 4, we show the results of this study for the particular case of a family of X-shaped dimers, composed of two ellipsoids touching near their 'equators'. The family is characterized by the twist angle ϕ between the two arms of the X.

The chemical potential of this species, in the twisted nematic, is shown as a function of ϕ in the figure. This may simply be obtained from the pair distribution function for ellipsoids in the simulated system: it is not necessary to introduce a chiral molecule explicitly. The curve is not symmetrical to the transformation between mirror-image forms of the dimer $\phi \leftrightarrow -\phi$, as can be seen; the difference between these two functions leads to an estimate of the helical twisting power (see figure) as a function of ϕ. We see that the most effective chiral dopants in this family have a twist angle somewhat higher than 45° (for X shapes, both $\phi = 0°$ and $\phi = 90°$ are non-chiral). The magnitudes of β observed here are roughly comparable with those seen in experiment. For example, a 1% solution of the dopant would produce an equilibrium helix pitch of the order of hundreds of molecular lengths. Needless to say, it would be very expensive to simulate a system of this size directly.

(*b*) *Dynamical properties*

Now we turn to the simplest dynamical property, the diffusion coefficient, which also gives us an example of simulation results encouraging the development and refinement of theory. In the nematic phase two separate diffusion coefficients $D_\parallel$ and $D_\perp$ describe translation respectively parallel and perpendicular to the director. Each is the time integral,

$$D_\parallel = \int_0^\infty \mathrm{d}t\, c_\parallel(t), \quad D_\perp = \int_0^\infty \mathrm{d}t\, c_\perp(t),$$

of an appropriate component of the centre-of-mass velocity autocorrelation function

$$c_\parallel(t) = \langle v_\parallel(0) v_\parallel(t) \rangle, \quad c_\perp(t) = \langle v_\perp(0)\, v_\perp(t) \rangle.$$

Here $v_\perp$ is either of the two cartesian components perpendicular to the director, while $v_\parallel$ lies along it. In the isotropic phase, there is just one function $c(t)$, and one diffusion coefficient D. These quantities have been measured, in simulations of the isotropic and nematic phases, for hard ellipsoids of revolution. It was observed (Allen 1990*b*) that, for highly non-spherical particles, $c(t)$ decays on two well-separated timescales in the isotropic phase (see figure 5).

In the nematic phase, for prolate ellipsoids, $c_\parallel(t)$ and $c_\perp(t)$ are both two-timescale functions, but are dramatically different in appearance: $c_\perp(t)$ decays very rapidly, having only a weak long-time component, while $c_\parallel(t)$ is predominantly a slowly decaying function (extending in some cases over many tens of collision times). Moreover, at densities just above the isotropic $\leftrightarrow$ nematic transition point, $D_\parallel$ rose to a plateau with increasing density, before resuming the normal monotonically

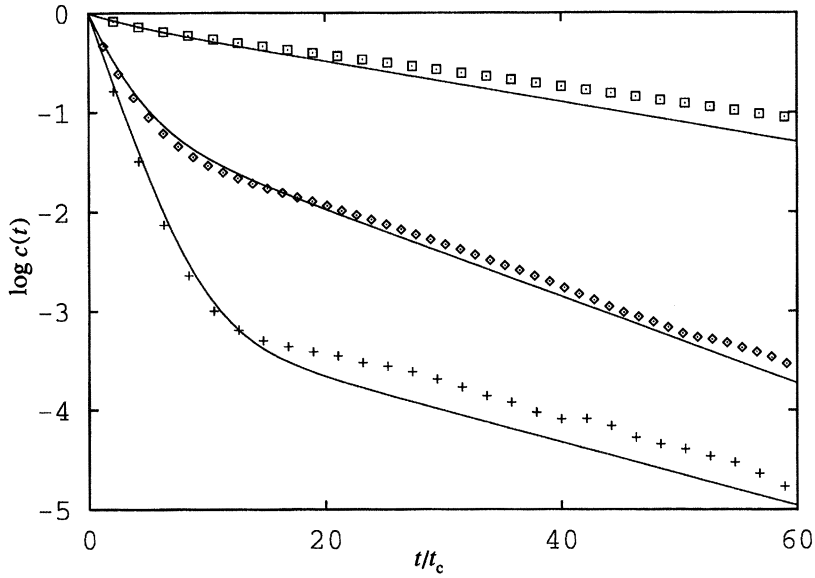

Figure 5. Normalized velocity autocorrelation functions, plotted on a logarithmic scale: $c(t)$ (diamonds) for $e = 10$ prolate ellipsoids, in the isotropic phase at $\rho^* = 0.25$; $c_\parallel(t)$ (squares) and $c_\perp(t)$ (plus signs) for $e = 10$ prolate ellipsoids, in the nematic phase at $\rho^* = 0.35$. The lines are the kinetic theory predictions (Tang & Evans 1993). The time t is measured in units of the mean time between collisions per particle t_c.

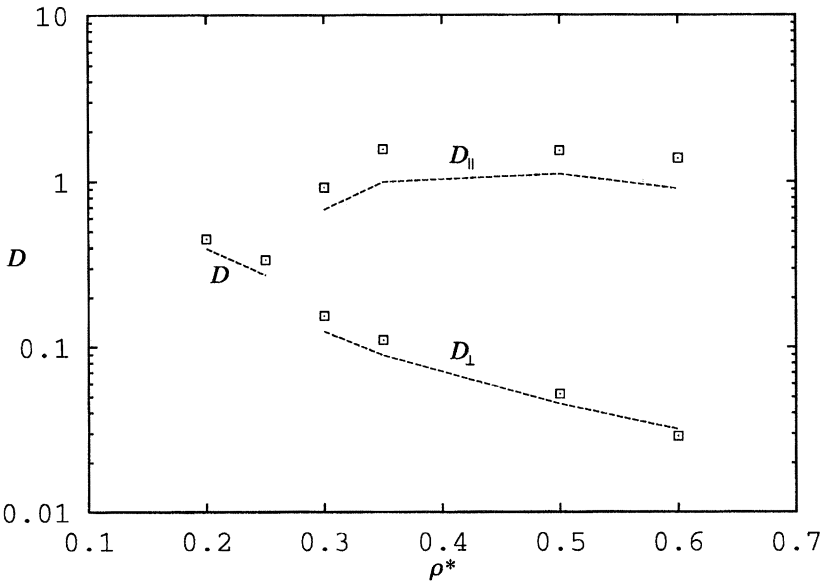

Figure 6. Diffusion coefficients D, $D_\parallel$, and $D_\perp$ for $e = 10$ prolate ellipsoids, plotted on a logarithmic scale, as functions of reduced density ρ^*. Points, simulation results; lines, kinetic theory (Tang & Evans 1993).

decreasing behaviour (see figure 6). For oblate particles, similar behaviour was seen, but with the roles of $c_\parallel(t)$ and $c_\perp(t)$ (and $D_\parallel$ and $D_\perp$) exchanged.

Until recently, there was no quantitative explanation of these results, even for densities where one might expect kinetic theory to be valid. Hess *et al.* (1991)

developed a theory based on relating the highly ordered system of ellipsoids to a reference system of hard spheres, by affine transformation. This correlated, very successfully, the anisotropy of diffusion, $(D_\parallel - D_\perp)/(D_\parallel + 2D_\perp)$ with the order parameter S and molecular shape e, but provided little insight into the microscopic origin of these effects. Very recently, a kinetic theory has been constructed (Tang & Evans 1993) for these highly elongated ellipsoids. At the heart of this approach is the expression of the velocity correlation functions above in terms of a set of friction coefficients, one for each of the basic relative orientations of the axis vector of the moving particle $\boldsymbol{u}$, the director $\boldsymbol{n}$, and the velocity vector $\boldsymbol{v}$. The friction coefficients themselves are calculated using a projection-operator approach for binary collisions, involving the distribution function for pairs at contact. This kinetic theory naturally leads to the two-timescale decay for the correlation functions, mentioned above. With only the order parameter S and the collision rate as input for the theory, and no adjustable parameters, the agreement with the simulation results is spectacularly good (see figures 5 and 6). This also illustrates that, for molecular systems, kinetic or 'Enskog' theory is not synonymous with single-exponential decay of the time correlations: the situation is more complicated, but can still be described perfectly adequately.

5. Conclusions

In this short paper, I have tried to show the current capabilities of computer simulation in this field, present some recent results, and point the way to the future. I have restricted my view to hard-particle simulations; this has excluded much interesting work on other simple models of liquid crystals (see, for example, Luckhurst *et al.* 1990; de Miguel *et al.* 1992; de Miguel *et al.* 1991) and other self-assembled systems (see, for example, Smit 1993, and references therein). Simulations of all these systems are just reaching the stage where they can be genuinely useful in calculating quantities of practical interest, as well as fulfilling the need to test out theories. One of the challenges over the next few years will be to conduct simulations of large-scale inhomogeneous systems, so as to look at defect structures and textures, behaviour near interfaces, and polymer liquid crystal phases, for example. Another challenge will be to study phase transitions in sufficient detail, and with sufficient precision, to compare with experiment. This remains an interesting and active area of research, which undoubtedly will grow as computers continue to increase rapidly in power.

The support of the Science and Engineering Research Council, through the provision of computer hardware and supercomputer time, and NATO, through a travel grant, is gratefully acknowledged. I have had helpful conversations and collaborations with many individuals, but should note especially my debt to Douglas Cleaver, Glenn Evans, Daan Frenkel, Carl Mason, Andrew Masters, Enrique de Miguel, Bela Mulder and Mark Wilson. Thanks are also due to Glenn Evans for providing a preprint of Tang & Evans (1993).

References

Allen, M. P. 1990*a* Computer simulation of a biaxial liquid crystal. *Liq. Cryst.* **8**, 499–511.

Allen, M. P. 1990*b* Diffusion coefficient increases with density in hard ellipsoid liquid crystals. *Phys. Rev. Lett.* **65**, 2881–2884.

Allen, M. P. 1993*a* Back to basics. In *Computer simulation in chemical physics* (ed. M. P. Allen & D. J. Tildesley). Dordrecht: Kluwer. (NATO Advanced Study Institute, Alghero, 1992.) *NATO ASI* C **397**, 49–92.

PHILOSOPHICAL TRANSACTIONS OF THE ROYAL SOCIETY A MATHEMATICAL, PHYSICAL & ENGINEERING SCIENCES

Allen, M. P. 1993*b* Calculating the helical twisting power of dopants in a liquid crystal by computer simulation. *Phys. Rev.* E. (In the press.)

Allen, M. P. & Frenkel, D. 1987 Observation of dynamical precursors of the isotropic-nematic phase transition by computer simulation. *Phys. Rev. Lett.* **58**, 1748–1750.

Allen, M. P. & Frenkel, D. 1988 Calculation of liquid crystal Frank constants by computer simulation. *Phys. Rev.* A **37**, 1813–1816.

Allen, M. P. & Frenkel, D. 1990 Calculation of liquid crystal Frank constants by computer simulation. *Phys. Rev.* A **42**, 3641. (Erratum.)

Allen, M. P. & Masters, A. J. 1993 Computer simulation of a twisted nematic liquid crystal. *Mol. Phys.* (In the press.)

Allen, M. P. & Tildesley, D. J. 1987 *Computer simulation of liquids*. Oxford: Clarendon Press.

Allen, M. P. & Wilson, M. R. 1989 Computer simulation of liquid crystals. *J. Comput. Aided Mol. Des.* **3**, 335–353.

Allen, M. P., Frenkel, D. & Talbot, J. 1989 Molecular dynamics simulation using hard particles. *Comp. Phys. Rep.* **9**, 301–355.

Allen, M. P., Evans, G. T., Frenkel, D. & Mulder, B. M. 1993 Hard convex body fluids. *Adv. Chem. Phys.* (In the press.)

Amos, M. D. & Jackson, G. 1992 Bonded hard sphere (BHS) theory for the equation of state of fused hard-sphere polyatomic molecules and their mixtures. *J. chem. Phys.* **96**, 4604–4618.

Binder, K. & Stauffer, D. 1987 A simple introduction to Monte Carlo simulation and some specialized topics. In *Applications of the Monte Carlo method in statistical physics* (ed. K. Binder), pp. 1–36. Berlin and Heidelberg: Springer-Verlag.

Ciccotti, G., Frenkel, D. & McDonald, I. R. (eds) 1987 *Simulation of liquids and solids*. Amsterdam: North-Holland.

Cleaver, D. J. & Allen, M. P. 1993 Computer simulation of liquid crystal films. *Mol. Phys.* (In the press.)

de Gennes, P. G. 1974 *The physics of liquid crystals*. Oxford: Clarendon Press.

de Miguel, E., Rull, L. F., Chalam, M. K. & Gubbins, K. E. 1991 Liquid crystal phase diagram of the Gay–Berne fluid. *Mol. Phys.* **74**, 405–424.

de Miguel, E., Rull, L. F. & Gubbins, K. E. 1992 Dynamics of the Gay–Berne fluid. *Phys. Rev.* A **45**, 3813–3822.

Eppenga, R. & Frenkel, D. 1984 Monte Carlo study of the isotropic and nematic phases of infinitely thin hard platelets. *Mol. Phys.* **52**, 1303–1334.

Frenkel, D. 1986 Free-energy computation and first-order phase transitions. In *Molecular dynamics simulation of statistical-mechanical systems* (ed. G. Ciccotti & W. G. Hoover), pp. 151–188. Amsterdam: North-Holland, for International School of Physics 'Enrico Fermi', Course XCVII.

Frenkel, D. 1987 Computer simulation of hard-core models for liquid crystals. *Mol. Phys.* **60**, 1–20.

Frenkel, D. 1988 Structure of hard-core models for liquid crystals. *J. Phys. Chem.* **92**, 3280–3284.

Frenkel, D. & Mulder, B. M. 1985 The hard ellipsoid-of-revolution fluid. 1. Monte Carlo simulations. *Mol. Phys.* **55**, 1171–1192.

Frenkel, D., Mulder, B. M. & McTague, J. P. 1984 Phase diagram of a system of hard ellipsoids. *Phys. Rev. Lett.* **52**, 287–290.

Frenkel, D., Lekkerkerker, H. N. W. & Stroobants, A. 1988 Thermodynamic stability of a smectic phase in a system of hard rods. *Nature, Lond.* **332**, 822–823.

Hansen, J.-P. & McDonald, I. R. 1986 *Theory of simple liquids*, 2nd edn. New York: Academic.

Heppke, G., Lötzsch, D. & Oestreicher, F. 1986 Chirale Dotierstoffe mit aussergewöhnlich hohem Verdrillungsvermögen. *Z. Naturf.* a **41**, 1214–1218.

Heppke, G., Kitzerow, H. S., Lötzsch, D. & Papenfuss, Ch. 1990 Blue phase mixtures exhibiting low fractions of a chiral compound. Experimental observation of some unusual properties. *Liq. Cryst.* **8**, 407–418.

Hess, S., Frenkel, D. & Allen, M. P. 1991 On the anisotropy of diffusion in nematic liquid crystals: test of a modified affine transformation model via molecular dynamics. *Mol. Phys.* **74**, 765–774.

PHILOSOPHICAL TRANSACTIONS OF THE ROYAL SOCIETY A MATHEMATICAL, PHYSICAL & ENGINEERING SCIENCES

Luckhurst, G. R., Stephens, R. A. & Phippen, R. W. 1990 Computer-simulation studies of anisotropic systems. XIX. Mesophases formed by the Gay–Berne model mesogen. *Liq. Cryst.* **8**, 451–464.

Mouritsen, O. G. 1984 *Computer studies of phase transitions and critical phenomena*. Berlin and Heidelberg: Springer-Verlag.

Onsager, L. 1949 The effects of shape on the interaction of colloidal particles. *Ann. N.Y. Acad. Sci.* **51**, 627–659.

Perram, J. W. & Wertheim, M. S. 1985 Statistical mechanics of hard ellipsoids. 1. Overlap algorithm and the contact function. *J. Comp. Phys.* **58**, 409–416.

Perram, J. W., Wertheim, M. S., Lebowitz, J. L. & Williams, G. O. 1984 Monte Carlo simulation of hard spheroids. *Chem. Phys. Lett.* **105**, 277–280.

Rebertus, D. W. & Sando, K. M. 1977 Molecular dynamics simulation of a fluid of hard spherocylinders. *J. chem. Phys.* **67**, 2585–2590.

Smit, B. 1993 Computer simulation of surfactants. In *Computer simulation in chemical physics* (ed. M. P. Allen & D. J. Tildesley). Dordrecht: Kluwer. (NATO Advanced Study Institute, Alghero, 1992.) *NATO ASI* C **397**, 461–472.

Somoza, A. M. & Tarazona, P. 1989 Frank elastic constants of a nematic liquid crystal of hard molecules. *Phys. Rev.* A **40**, 6069–6076. (At the time of publication the erratum of Allen & Frenkel (1990) had not appeared. This changes the comparison of simulation and theory in this paper.)

Stroobants, A., Lekkerkerker, H. N. W. & Frenkel, D. 1986 Evidence for smectic order in a fluid of hard parallel spherocylinders. *Phys. Rev. Lett.* **57**, 1452–1455.

Tang, S. & Evans, G. T. 1993 Self diffusion in isotropic and nematic phases of highly elongated hard particles. *J. chem. Phys.* **98**, 7281–7288.

Tjipto-Margo, B. & Evans, G. T. 1990 The Onsager theory of the isotropic–nematic liquid crystal transition: incorporation of the higher virial coefficients. *J. chem. Phys.* **93**, 4254–4265.

Tjipto-Margo, B., Evans, G. T., Allen, M. P. & Frenkel, D. 1992 Elastic constants of hard and soft nematic liquid crystals. *J. phys. Chem.* **96**, 3942–3948.

Veerman, J. A. C. & Frenkel, D. 1990 Phase diagram of a system of hard spherocylinders by computer simulation. *Phys. Rev.* A **41**, 3237–3244.

Veerman, J. A. C. & Frenkel, D. 1992 Phase behavior of disklike hard-core mesogens. *Phys. Rev.* A **45**, 5632–5648.

Vieillard-Baron, J. 1972 Phase transitions of the classical hard ellipse system. *J. chem. Phys.* **56**, 4729–4744.

Vieillard-Baron, J. 1974 The equation of state of a system of hard spherocylinders. *Mol. Phys.* **28**, 809–818.

Whittle, M. & Masters, A. J. 1991 Liquid crystal formation in a system of fused hard spheres. *Mol. Phys.* **72**, 247–265.

Widom, B. 1963 Some topics in the theory of fluids. *J. chem. Phys.* **39**, 2808–2812.

Wilding, N. B. & Bruce, A. D. 1992 Density fluctuations and field mixing in the critical fluid. *J. Phys. Cond. Matter* **4**, 3087–3108.

Wilson, M. R. & Allen, M. P. 1993 A computer simulation study of liquid crystal formation in a semi-flexible system of linked hard spheres. *Mol. Phys.* (In the press.)

Zannoni, C. 1979 Computer simulation. In *The molecular physics of liquid crystals* (ed. G. R. Luckhurst & G. W. Gray), pp. 191–200. London: Academic Press.

Zarragoicoechea, G. J., Levesque, D. & Weis, J. J. 1992 Monte Carlo study of dipolar ellipsoids. 2. Search for an isotropic nematic phase transition. *Mol. Phys.* **75**, 989–998.

Zhang, Z., Mouritsen, O. G. & Zuckermann, M. J. 1992 Weak first-order orientational transition in the Lebwohl–Lasher model for liquid crystals. *Phys. Rev. Lett.* **69**, 2803–2806.

PHILOSOPHICAL TRANSACTIONS OF THE ROYAL SOCIETY A MATHEMATICAL, PHYSICAL & ENGINEERING SCIENCES